

RECORDING OF THE THERMAL EVOLUTION OF LIMESTONES UNDERGOING EXPERIMENTAL ACCELERATED AGEING TESTS

Ronan L. Hébert¹, Matthieu Angeli², Eric Doehne³ [and](#) Sandra Dochez⁴

¹ *G.E.C., Université de Cergy-Pontoise, 95031 Cergy cedex, France*

² *Department of Geosciences, University of Oslo, 0316 OSLO, Norway*

³ *Conservation Sciences, Pasadena, CA91103-3263, USA*

⁴ *INERIS, Parc Technologique Alata, 60550 Verneuil en Halatte, France*

Abstract

Sodium sulfates are widely regarded as the most destructive salts for porous stone, concrete and brick. Thenardite (Na_2SO_4), mirabilite ($\text{Na}_2\text{SO}_4 \cdot 10\text{H}_2\text{O}$) and heptahydrate ($\text{Na}_2\text{SO}_4 \cdot 7\text{H}_2\text{O}$) are the common phases that occur under surface conditions. The heptahydrate phase has been largely neglected in most modern work about salt weathering. However, several recent publications suggest that it could play an important role in geochemical and planetary processes. Therefore its role in the $\text{Na}_2\text{SO}_4\text{-H}_2\text{O}$ system should be clarified.

We present here results of accelerated ageing experiments performed on samples of a micritic limestone under two different ambient temperatures: 20°C (i.e. below the upper limit of metastability of the heptahydrate), and 30°C (i.e. above this limit and also below the upper limit of stability of mirabilite). Thermocouples were placed into the samples in order to follow the evolution of the temperature of the stones during the weathering tests. This method allows the recording of exo- and endothermic reactions that are linked to physicochemical processes, such as crystallization, wetting, evaporative cooling, etc.

The experiments show significant differences in the pattern and degree of damage. In the experiment at 20°C, the loss of material is noticeable, and occurs as crumbling and scaling. In the experiment at 30°C, we observe just efflorescence with no visible loss of material. The recorded thermal evolution is also different for the two experiments, which provides some clues as to the different physicochemical processes occurring in each situation, depending on the ambient temperature.

Keywords: heptahydrate, mirabilite, sodium sulfates, accelerated ageing test

1. Introduction

Sodium sulphates are widely regarded as the most destructive salts for porous stones, and other building materials such as concrete or brick (Goudie et al. 1997). It is important to fully understand their crystallization process in porous networks and, in the future, to find ways to prevent or limit their damage to porous materials.

Anhydrous sodium sulphates (i.e. Na_2SO_4) occur in several polymorphic forms labeled I-V (Kracek 1929; Eysel 1973; Rasmussen et al. 1996, Rodriguez-Navarro et al. 2000). Phases I, II and IV are high temperature polymorphs (I >270°C and II >225°C). Phase IV is poorly known (e.g. Rasmussen et al. 1996; Rodriguez-Navarro et al. 2000) but it is considered to be metastable with a small temperature range of existence (210-220°C). Phase V, known as thenardite (Thn), is the stable phase at low temperature (i.e. close to ordinary temperature), low relative humidity and is the naturally occurring

mineral. Phase III is metastable and is frequently observed during evaporation of a sodium sulphate solution (Amirthalingam et al. 1977). Note that there is no indication that phases I, II and IV occur as metastable phases close to ambient temperatures (Steiger and Asmussen, 2008).

Sodium sulphates can also occur as hydrates: the decahydrate (Mirabilite: $\text{Na}_2\text{SO}_4 \cdot 10\text{H}_2\text{O}$; Mir), which is stable below 32.4°C (Figure 1) and the heptahydrate (unnamed, $\text{Na}_2\text{SO}_4 \cdot 7\text{H}_2\text{O}$; SS7), which is metastable below 24°C (Figure 1). These limited temperatures of stability (for Mir) and metastability (for SS7) correspond to peritectic temperatures where the hydrates undergo an incongruent melting to Thn. These temperatures are higher when peritectic reactions produce anhydrous form III (34.06°C for mirabilite, 28.25°C for heptahydrate; Steiger and Asmussen 2008). Although it is known since the middle of the 19th century (Loewel 1850), the heptahydrate has been largely neglected in almost all modern works about salt weathering. Heptahydrate has been recently the subject of abundant publication (e.g. Genkinger and Putnis 2007; Hamilton et al. 2008; Hamilton and Hall 2008; Steiger and Asmussen 2008; Espinosa Marzal and Scherer 2008; Derluyn et al. 2011; Saidov et al. 2012) suggesting that it very likely plays an important role into geochemical and planetary processes, and therefore it should be reconsidered in the $\text{Na}_2\text{SO}_4\text{-H}_2\text{O}$ system.

Anhydrous Na_2SO_4 (III and V) can form directly upon evaporation of a sodium sulfate solution above 32.4°C (Amirthalingen et al. 1977) but also by dehydration of mirabilite (Rodriguez-Navarro et al. 2000). Hydrated Na_2SO_4 can form upon evaporation of a sodium sulfate solution below 32.4°C , as well as upon cooling of the same solution. The relationship between the heptahydrate and the decahydrate is not straightforward. There are several studies that show that mirabilite rarely forms directly from supersaturated sodium sulfate solutions (in the absence of seed crystals), and that the first solid to form is the metastable heptahydrate when cooling or evaporating a supersaturated sulfate sodium solution (e.g. Loewel 1850; Hartley 1908; Genkinger and Putnis 2007; Rijniens et al. 2005; Espinosa Marzal and Scherer 2008; Pel et al. 2010; Derluyn et al. 2011; Saidov et al. 2012).

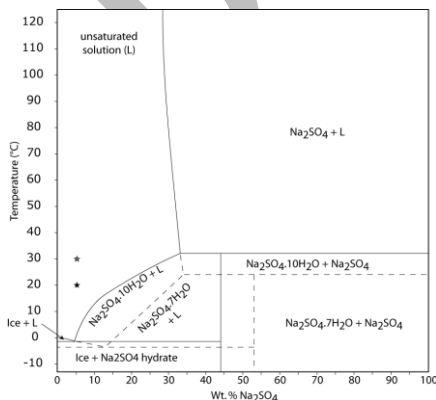


Figure 1. Phase diagram of the $\text{Na}_2\text{SO}_4\text{-H}_2\text{O}$ system. Stars represent the concentration and Temperature for the two experiments.

The destructive effect of sodium sulfates in porous media is attributed to Mir (rather than Thn) especially when forming from highly supersaturated solution originating from the rapid dissolution of Na_2SO_4 (Chatterji and Jensen 1989; Flatt 2002;

Tsui et al. 2003; Steiger and Asmussen 2008). SS7, according to Rijniers et al. (2005) is considered to be harmless.

Several studies (e.g. Rodriguez-Navarro and Doehne 1999; Flatt 2002; Scherer 2004; Angeli et al. 2010) have shown that temperature plays a major role on salt weathering of sedimentary rocks. For this reason, we present in this study some results of accelerated ageing experiments performed on samples of a detritic limestone under two different ambient temperatures: 20°C, which is below the upper limit of metastability of SS7, and 30°C, which is above this limit and also below the upper limit of stability of Mir. The goal of this experimental study is to evaluate the possible role of SS7 in the damage of porous material by sodium sulfate crystallization. The originality of this study is that we placed thermocouples into the samples in order to follow the evolution of the temperature of the stones during the accelerated ageing tests. We discuss the temperature curves for each phase of the cycle with the aim of understanding the processes that occur and that are responsible for the damage observed in the two experiments.

2. Material and methods

2.1 Material

Cubic samples (7 cm/side) of a lutetian-aged limestone from the Paris Basin commercially known as “Roche fine” have been used in this study. This rock has been chosen for several reasons: it is relatively homogenous from one sample to another, it has been widely used for construction in Paris (historic buildings and monuments), it is one of the stones required for use in restoration and construction in the protected areas of the “Ile de France” region, and it is also the rock that has been used in previous experiments from which the current study originated (e.g. Angeli et al. 2010). Roche fine is a fine-grained detritic limestone made of calcite (90%) and quartz (10%) with a very low tensile strength (1.5 MPa), a high porosity (37, 2%) with two pore entry sizes (mainly around 20 µm, and another one between 0.03 to 5 µm). Complete hydromechanic properties are available in Angeli et al. 2007.

We used four samples per experiment. All samples undergo several cycles of washing by immersion in demineralized water at room temperature for 6 hours and drying at 105°C until constant weight, in order to remove any possible natural occurrence of soluble salts in the stone. A single thermocouple is placed in each cube at the center of the sample. The drill hole used to insert the thermocouple is filled up with a mixture of lime and limestone powder resulting from the drilling of the sample.

The thermocouples (type K) are connected to a thermal acquisition station (Agilent 34970A) with 22 recording channels. The acquisition station is connected to a personal computer using ® Agilent BenchLink Data Logger software for programming the thermal station and recording data. According to the manufacturer, the accuracy of measurement is $\pm 0.5^\circ\text{C}$.

2.2 Methodology

The samples are subjected to 24 hours accelerated ageing cycles modified from the EN 12370 standard test. The cycles consist of three stages.

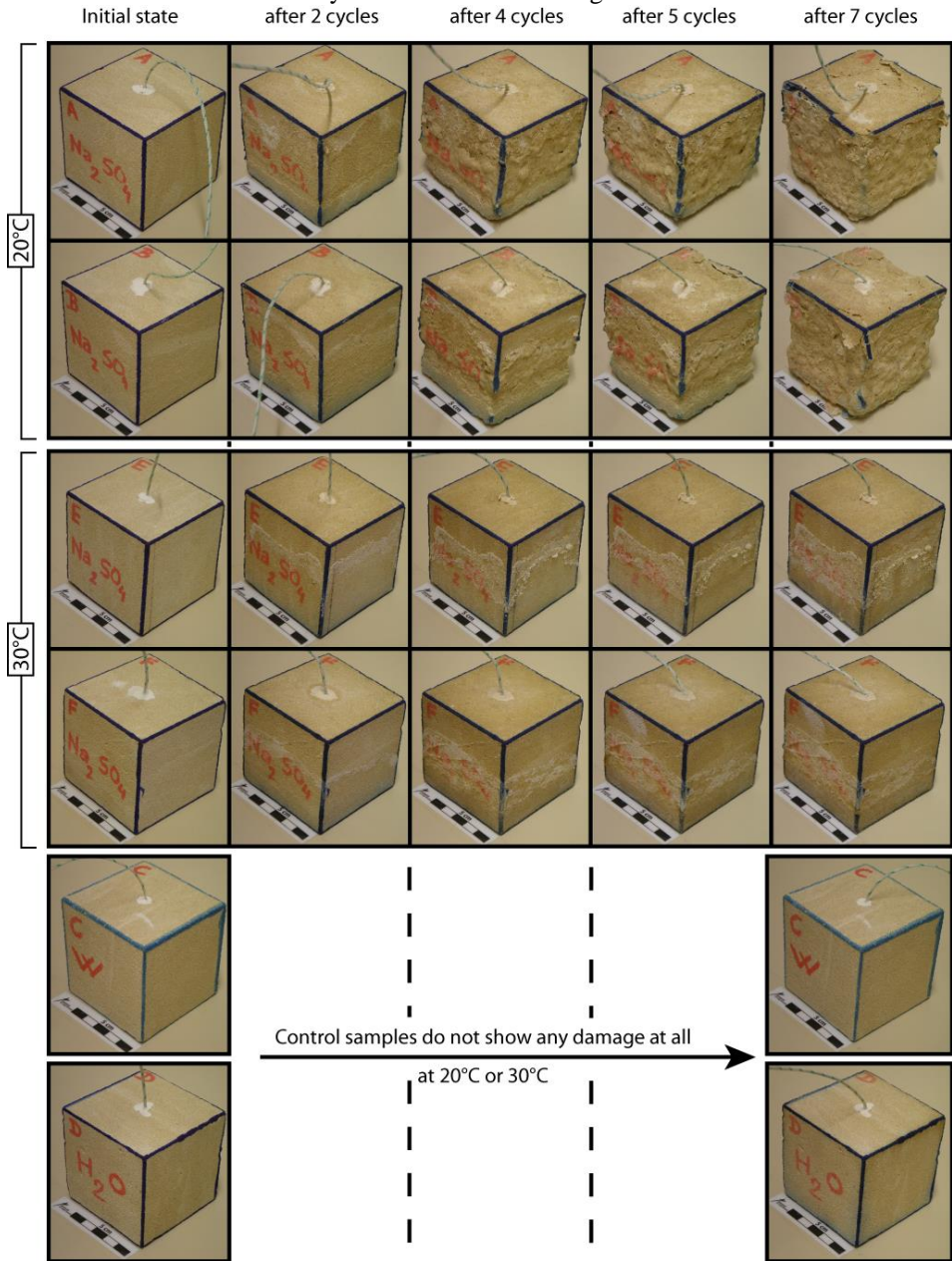


Figure 2. Macroscopic evolution of the samples during the accelerated ageing cycles

- (i) 2 hours imbibition at “ambient” temperature; the 4 samples are placed in a cooled incubator (® LMS 303NP) where the temperature is fixed at 20°C or 30°C according to the experiment. 2 samples soak in approximately 0.5 mm height of a sodium sulfate solution of 5.5 weight % Na₂SO₄; the two other samples are used for control and comparison. For one of these samples, the sodium sulfate solution is substituted with demineralized water, and for the other one there is no imbibition solution at all. Each sample is placed into an individual box that is supplied with solution by a system of drop by drop, and with an overflow in order to keep the level of solution constant. The solutions are stored at ambient temperature in the incubator.
- (ii) 16 hours of drying. All the samples are placed in a drying oven (®memmert UE600) at 105°C.
- (iii) 6 hours of cooling; the samples are replaced into the cooling incubator with fixed temperature so that they return to their initial “ambient” temperature, i.e. respectively 20°C and 30°C .

The samples are weighed and photographed after each stage. Seven full cycles have been performed during which the temperature was recorded every 3 minutes.

3. Results

3.1 Rock decay vs. cycle

Figure 2 shows the different samples at the different stages of the 7 cycles. The reference samples do not show any damage after 7 cycles. The weight monitoring (Figure 3) confirms that their weight remains constant through the full experiment independently of the ambient temperature, suggesting that the limestone is inert with respect to demineralized water.

Samples subject to Na₂SO₄ solution at 20°C show intense damage starting with efflorescence (from cycle 1), then contour scaling (from cycle 3), crumbling, and desquamation leading to an important change of shape. The distribution of the damage is heterogeneous. An important loss of material is observed at the bottom of the samples from cycle 4. It seems related to a granular decohesion as suggested by the presence of loose material at the end of the imbibition stage (starting from cycle 3). Vertical faces are more affected by crumbling and the top of the samples by cracking and desquamation. In contrast, samples in exp 30 do not present any major damage but just efflorescence that starts to occur as soon as cycle 1 and increases with continuing cycles. The monitoring of sample weight during cycles (Figure 3a) shows consistent results with the shape evolution described above. All the samples undergo a similar weight increase during the two first cycles, but the evolution differs from cycle 3. Indeed, samples in exp 30 show a continuous and progressive weight gain, while samples in exp 20 show a smaller weight increase during the third cycle, before undergoing weight decrease from cycle 4. All these results are consistent with previous research (Price 1978; Angeli et al. 2007, 2010).

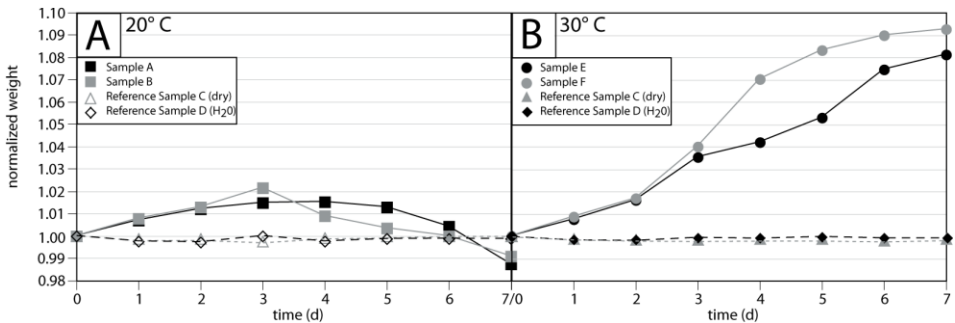


Figure 3. Weight evolution of the samples in the dry state at 20°C (A) and 30°C (B)

3.2 Temperature evolution of the control samples

The temperature curves for the "dry" reference samples are shown on Figure 4. The curves are very regular. They show in particular a constant and high heating rate of the samples during drying until reaching a plateau at 105°C. Then a progressive and constant decrease of temperature is observed during cooling until reaching the ambient temperature where a second plateau is observed. This indicates that the studied limestone presents an inert behavior with respect to temperature. Temperature curves are consistent with the model of heat diffusion through the rock.

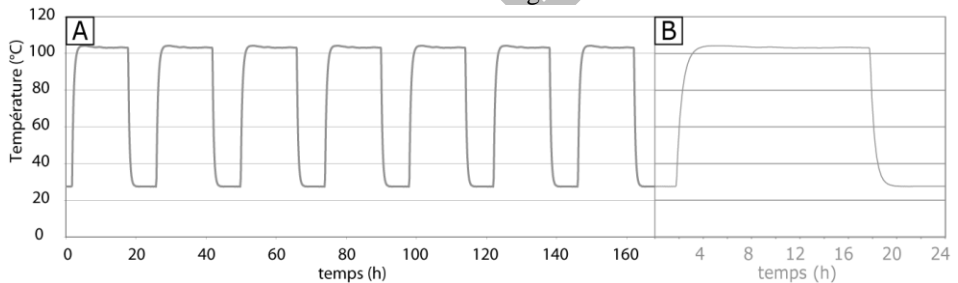


Figure 4. Temperature evolution of the "dry" reference during the 7 cycles (A), and for a single cycle of 24 hours (B). The Temperature profile is in exp20.

The temperature curves of reference samples undergoing imbibition by demineralized water (Figure 5) are also very regular and similar whatever the ambient temperature. During wetting, the temperature of the sample decreases (-8°C in exp 20, and -6°C in exp 30). This is due to the evaporative cooling. The drying period is characterized by a variation of the heating rate. First, we observe a rapid increase of temperature until a sort of plateau at $\sim 59^{\circ}\text{C}$, then a deceleration of the temperature increase up to an inflection point at $\sim 85^{\circ}\text{C}$ where it becomes more rapid again (but not as much as the beginning of drying) until reaching the final plateau at 105°C . The variation of the heating rate indicates the occurrence of two endothermic reactions, the first, requiring more energy than the second. The first, leading to the $\sim 59^{\circ}\text{C}$ plateau, would correspond to the departure of water on the surface as well as the water trapped in the $20\ \mu\text{m}$ size entry pores, the second (inflection point at 85°C) would correspond to the departure of the water trapped within the small entry size pores. Cooling is characterized by a rapid, progressive and continuous return to ambient temperature.

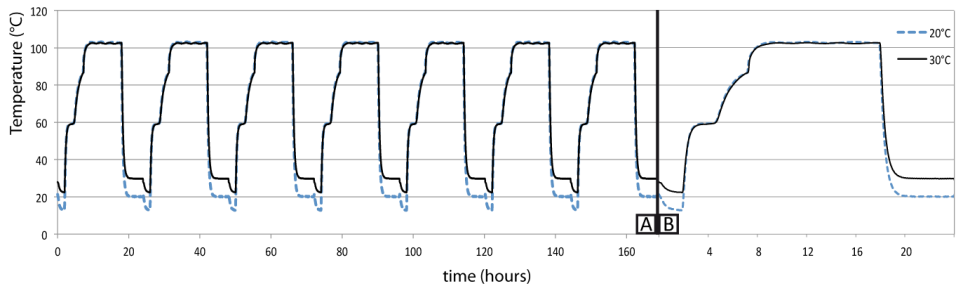


Figure 5. Temperature evolution of the reference samples undergoing imbibition by demineralized water during the 7 cycles (A), and for a single cycle of 24 hours (B).

3.3 Temperature evolution of the samples subject to salt weathering

Before discussing the different stages of the cycles for each experiment, it is worth noting that the first cycle is always very different from the following cycles that are more repetitive, as if the first cycle is a transitory phase (Figure 6). The difference between cycle 1 and following cycles is the absence of salt in the porous network of the stone at the beginning of the imbibition. Therefore, cycle one will not be discussed in this study, in particular the drying stage on which we cannot rely.

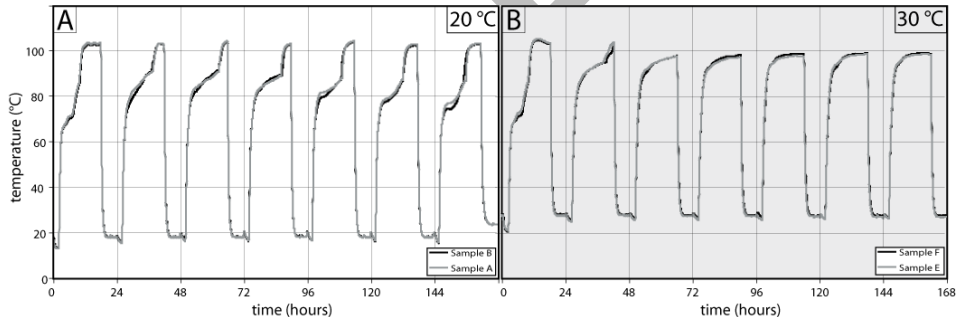


Figure 6. Temperature evolution of samples undergoing accelerated aging cycles with sodium sulfates at 20°C (A) and 30°C (B).

3.3.1 Evolution of the temperature during imbibition

The first imbibition is characterized by a significant temperature decrease of several degrees ($\sim -5.5^{\circ}\text{C}$ in exp 20, and in exp 30) that lasts all along this stage. From cycle 2, the imbibition is characterized first by a temperature rise immediately followed by a fall of temperature. The temperature rise matches with the hydration of the system, which leads to the dissolution of the salts (Thn?) formed during former drying period. Depending on the salinity and temperature, the rehydration of the system can also correspond with the formation of hydrates. This interpretation is consistent with the lack of temperature increase during the first imbibition as there is no salt in the sample at the beginning of the experiment. Temperature decrease is due to evaporative cooling as in the first imbibition.

It is worth noting that the temperature rise is more important in exp 20 than that in exp 30 (more Mir crystallized). In a similar way, the temperature decrease due to evaporative cooling increases progressively with cycles in exp 20 whilst it decreases in

exp 30. Then several chemical phenomena occur during this part of the cycle, which correspond to the major (if not single) phase of damage.

3.3.2 Evolution of the temperature during drying

The drying behavior is very different during the first cycle than during the subsequent cycles. In exp 20, the drying period can be divided into 4 stages: (i) rapid heating, similar to what happens on the reference samples; (ii) slower heating period; (iii) rapid heating again, same velocity as in first stage; and (iv) temperature step at 105°C (plateau). The differences in the drying period all occur during the lower velocity heating. Comparing this velocity to the dry sample velocity shows that an endothermic reaction occurs at this moment, and that this reaction draws its energy from the heat of the oven. There are several features to be noted:

- the drying velocity decreases progressively from the 2nd cycle to the 5th cycle
- from the 5th cycle to the end, the temperature remains constant for a period and then starts to increase again
- the duration of the step at 105°C increases at every cycle

It appears that this endothermic reaction requires more and more energy at every cycle, showing that there are more and more reactants (salts) at every cycle. Since the salt content in the sample increases at every cycle, we can assume that the hydrate (Mir?) production during the imbibition (damaging) stage increases accordingly. Thus, there is a larger amount of hydrate to dehydrate.

From this point, the "evaporation duration" is defined as the time necessary to reach 105°C. It is approximately the amount of time needed to remove all the water in the sample. The evaporation duration increases until the appearance of decay. This suggests that the efflorescence partially blocks the pores at the surface, thus reducing the evaporative surface. Once the decay starts at cycle 4, the evaporation duration is progressively reduced. This increase in the drying velocity shows that the decay of the surface creates cracks and/or reduces the sealing efficiency of the salt crust.

The drying stage in exp 30 is much simpler. The initial drying velocity is similar to the reference sample until water starts to evaporate. Then, the evaporation velocity starts to decrease, which corresponds to the evaporation of water in the sample and the precipitation of Thn. The remaining bulk (stone + Thn) is then heated to 105°C. Apparently very little of the damaging hydrated phase occurred during imbibition and no damage has been observed in the sample after 7 cycles. Mir is a mineral that grows easily but nucleates very seldomly. A possible explanation for the lack of Mir crystallization in exp 30 could be that since Mir is difficult to nucleate (Hartley et al. 1908), it could need an intermediate heptahydrate phase nucleation to be initiated and later grow from the heptahydrate nucleus as saturation increases by evaporation or cooling (but temperature is over the limit of metastability of SS7 in this precise case). Another explanation (according to the phase diagram) is that until supersaturation is reached, no Mir can precipitate, and once it has, only a small amount of Mir crystallizes.

3.3.3 Evolution of the temperature during cooling

The temperature evolution during cooling is more straightforward. It requires about 2 hours for each sample to return to its ambient temperature from the peak of temperature achieved at the end of the drying stage (Figure 6). This cooling is fast (~50°C/hour) at the beginning, and slows down when approaching ambient temperature.

We can consider that all the samples have returned to their ambient T after 2 hours and therefore, they do not undergo further temperature variation until the beginning of next cycle.

4. Conclusions

After 7 complete cycles of 24 hours, the samples at 20°C and 30°C show different damage patterns as well as different temperature curves. It illustrates the difficulty of completely removing the water from the rock under certain conditions--as illustrated by the impossibility of reaching 105°C at the end of the drying period for the experiment at 30°C. This suggests that the crystallization of salts can fill the pore entries, trapping sodium sulfate solutions or more likely hydrated phases. It requires either more energy or a longer period of drying to release water from the samples. This result raises questions about the accuracy and the relevance of the standard stone durability tests.

The evaporative cooling phenomenon shows that imbibition is a favorable stage for the precipitation of sodium sulfate hydrates, especially if the concentration of the solution is close to supersaturation. Evaporation during this stage can trigger nucleation, and the cooling favors crystal growth.

The temperature profiles of this experiment do not enable the positive identification of two different hydrates. Supersaturation is achieved sooner at 20 than 30°C, which drives more hydrates to precipitate during imbibition. In addition, as complete dehydration of the sample is not reached in exp 30, there is less (or even no) Thn to transform during imbibition. Therefore, the current results do not allow an estimate of the role of SS7 in the weathering of rocks by sodium sulfates.

Finally, this study shows that recording temperature cycles can provide a simple and inexpensive method that enables monitoring exo/endothemic physico-chemical processes such as phase crystallization. It can be useful to identify mineral precipitation, sequences of crystallization and the important stages (wetting, evaporation, cooling) that are involved in rock damage.

References

- Amirthalingam V, Karkhanavala M, & Rao U. 1977. 'Topotaxic phase change in Na_2SO_4 ', *Acta Crystallographica*, **33**:522-523.
- Angeli M., Bigas J.P., Benavente B., Menendez B., Hébert R. & David C. 2007. 'Salt crystallization in pores: quantification and estimation of damage', *Environmental Geology*, **52**:205-213.
- Angeli M., Hébert R., Menéndez B., David C. and Bigas J.P. 2010. 'Influence of temperature and salt concentration on the salt weathering of sedimentary stones with sodium sulphate', *Engineering Geology*, **115**:193-199.
- Chatterji, S., and Jensen, A.D. 1989. 'Efflorescence and breakdown of building materials', *Nordic Concrete Research*, **8**:56-61.
- Derluyn H., Saidov T. A., Espinosa-Marzal R. M., Pel L., and Scherer G. W. 2011. 'Sodium sulfate heptahydrate I: The growth of single crystals', *Journal of Crystal Growth*, **329**(1):44-51.
- EN 12370. 1999. Natural stone test methods - Determination of resistance to salt crystallisation.
- Espinosa Marzal R. M., and Schere, G. W. 2008. 'Crystallization of sodium sulfate salts in limestone', *Environmental Geology*, **56**(3-4):605-621.

- Eysel W. 1973. Crystal chemistry of the system $\text{Na}_2\text{SO}_4\text{-K}_2\text{SO}_4\text{-K}_2\text{CrO}_4\text{-Na}_2\text{CrO}_4$ and of the glaserite phase', *American Mineralogist*, **58**:736-747.
- Flatt, R. J. 2002. 'Salt damage in porous materials: how high supersaturations are generated', *Journal of Crystal Growth*, **242**:435-454.
- Genkinger S and Putnis, A. 2007. 'Crystallization of sodium sulphate: supersaturation and metastable phases', *Environmental geology*, **52**:329-338.
- Goudie, A., Viles, H. 1997. *Salt Weathering Hazards*. Chichester : Wiley.
- Hamilton, A., and Hall, C. 2008. 'Sodium sulfate heptahydrate: a synchrotron energy-dispersive diffraction study of an elusive metastable hydrated salt', *Journal Of Analytical Atomic Spectrometry*, **23**(6):840-844.
- Hamilton, A., Hall, C., and Pel, L. 2008. 'Sodium sulfate heptahydrate: direct observation of crystallization in a porous material', *Journal of Physics D: Applied Physics*, **41**(21):212002.
- Hartley, H., Jones, B. M., Hutchinson, G. A., and Jones, G. 1908. 'The Spontaneous Crystallization of Sodium Sulfate Solutions', *Journal of the Chemical Society Transactions*, **433**(7021):825-833.
- Kracek, 1929. *Int. Critical Tables*, **3**:371.
- Loewel, H. 1850. 'Observations sur la sursaturation des dissolutions salines', *Annales de Chimie et de Physique*, **29**:62-127.
- Pel, L., Saidov, T.A., Espinosa-Marzal, R.M. and Scherer, G.W. 2010. 'The formation of meta-stable sodium sulfate heptahydrate in porous materials as studied by NMR', *Proceedings of the MEDACHS10, 28-30 April 2010, La Rochelle, France*.
- Price, C. A. 1978. 'The use of the sodium sulphate crystallisation test for determining the weathering resistance of untreated stone'. In *Altération et protection des monuments en pierre: Colloque international: Paris, du 5 au 9 juin*.
- Rijniers, L. A., Huinink, H. P., Pel, L., and Kopinga, K. 2005. 'Experimental evidence of crystallization pressure inside porous media', *Physical Review Letters*, **94**(7): 075503.
- Rodriguez-Navarro, C., and Doehne, E. 1999. 'Salt weathering: influence of evaporation rate, supersaturation and crystallization pattern', *Earth Surface Processes and Landforms*, **24**(3):191-209.
- Rodriguez-Navarro, C., Doehne, E., and Sebastian, E. 2000. 'How does sodium sulfate crystallize ? Implications for the decay and testing of building materials', *Cement and Concrete Research*, **30**(10):1527-1534.
- Scherer G. 2004. 'Stress from crystallization of salt', *Cement and Concrete Research*, **34**:1613-1624.
- Steiger, M., & Asmussen, S. 2008. 'Crystallization of sodium sulfate phases in porous materials: The phase diagram $\text{Na}_2\text{SO}_4\text{-H}_2\text{O}$ and the generation of stress', *Geochimica et Cosmochimica Acta*, **72**(17):4291-4306.
- Saidov T., Espinosa-Marzal, R., Pel, L. and Scherer, G. 2012. 'Nucleation of sodium heptahydrate on mineral substrates studied by nuclear magnetic resonance', *Journal of Crystal Growth*, **338**:166-169.
- Tsui, N., Flatt, R. J., & Scherer, G. W. 2003. 'Crystallization damage by sodium sulfate', *Journal of Cultural Heritage*, **4**(2):109-115.